

Microporous Polypropylene Sheets Containing Polymethylsilsesquioxane Filler

SATOSHI NAGŌ* and YUKIO MIZUTANI

Tokuyama Soda Co., Ltd., Tokuyama-City, 745 Japan

SYNOPSIS

Microporous sheets were prepared by biaxially stretching composite nonporous sheets composed of microspherical polymethylsilsesquioxane particles encased in polypropylene. The structural and physical property studies of the sheets obtained thereby show that the porosity, pore-size distribution, and the tortuosity vary with the average diameter of the encased particles as expected on the basis of theory. © 1993 John Wiley & Sons, Inc.

INTRODUCTION

It is well known¹⁻⁶ that microporous materials (films, sheets, or membranes) are very useful in separation technology.¹⁻⁴ We have reported^{5,6} on nonporous composite sheets composed of inorganic filler such as CaCO₃ or SiO₂ encased in polypropylene (PP). The resultant microporous PP sheets have interesting properties: They are dry and soft to the touch and have high porosity that affords good permeability to gas and water vapor, but not to liquid water.⁷⁻¹¹ This article reports the preparation of microporous sheets made by biaxially stretching PP sheets containing spheric polymethylsilsesquioxane fillers with narrow particle-size distributions to produce the corresponding microporous composite sheets, the macrostructured architecture of which is highly reproducible.

EXPERIMENTAL

Materials

The PP used was PN-120 (MFI, 1.2) from Tokuyama Soda Co. The polymethylsilsesquioxane fillers (commercial name, Trefil) were obtained from Dow Corning Toray Silicone Co. The particle sizes and

scanning electron micrographs of these particles are shown in Table I and Figure 1, respectively. Polybutadiene (polymerization degree, 1000; GI-1000 from Nippon Soda Co.) was used as an additive. The antioxidant admixed therein was 2,6-di-*t*-butyl-4-methylphenol of commercial grade.

Preparation of Microporous PP sheets

A premixed mixture of powdered PP (42 parts by weight), polymethylsilsesquioxane (56 parts) containing an additive and antioxidant (2 parts) was extruded at 230°C and pelletized with the aid of an extruder of tandem type from Nakatani Machine Co. The pellets obtained thereby were extruded at 230°C through a flat die attached on an uniaxial extruder from Iwamoto Manufacturing Co.

The sheet obtained thereby was stretched in the machine direction (MD) using two pairs of rollers operating in its shearing mode (stretching ratio, ×4). The sheets were then stretched at 120°C in the transverse direction (TD) with the aid of a biaxial stretching machine of pantograph type (Type I) purchased from Brückner Co. (stretching ratio, ×2) to produce the microporous sheets that were examined as described below.

Scanning Electron Microscopy (SEM)

The surface and cross section of microporous PP sheets were observed with the aid of an electron microscope, type JSM-T-220 from JEOL Ltd.

* To whom correspondence should be addressed.

Table I Properties of the Filler

No.	Mean Particle Size (μm)	Dispersion Degree of Particle Size (%)	Specific Gravity (g/cm^3)
1	2.0	4	1.32
2	1.3	10	1.32
3	0.8	14	1.32

Porosity

Apparent specific gravity (g/cm^3) was measured by a buoyancy method in water and the porosity was calculated using the following equation:

Porosity (ϵ)

$$\begin{aligned} &= \text{void volume/volume of porous sheet} \\ &= [(d_0 - d)/d_0] \times 100 \end{aligned} \quad (1)$$

where d_0 and d are specific gravity of the base sheet and the microporous sheet, respectively.

Pore-size Distribution

Pore-size distribution was measured using a mercury porosimeter, type 1500 from Carlo Erba Co.

Maximum Pore Size

The sample impregnated with methanol was set into a cell as shown in Figure 2(B). A small amount of methanol was filled over the sample surface and N_2 gas pressure was increased at the rate of $1 \text{ kg}/\text{cm}^2$ per min.

When three continuous bubbles were generated through the sample, N_2 gas pressure (P_j) was measured. Next, maximum pore size (D_{max}) was calculated by the following equation (ASTM F-316):

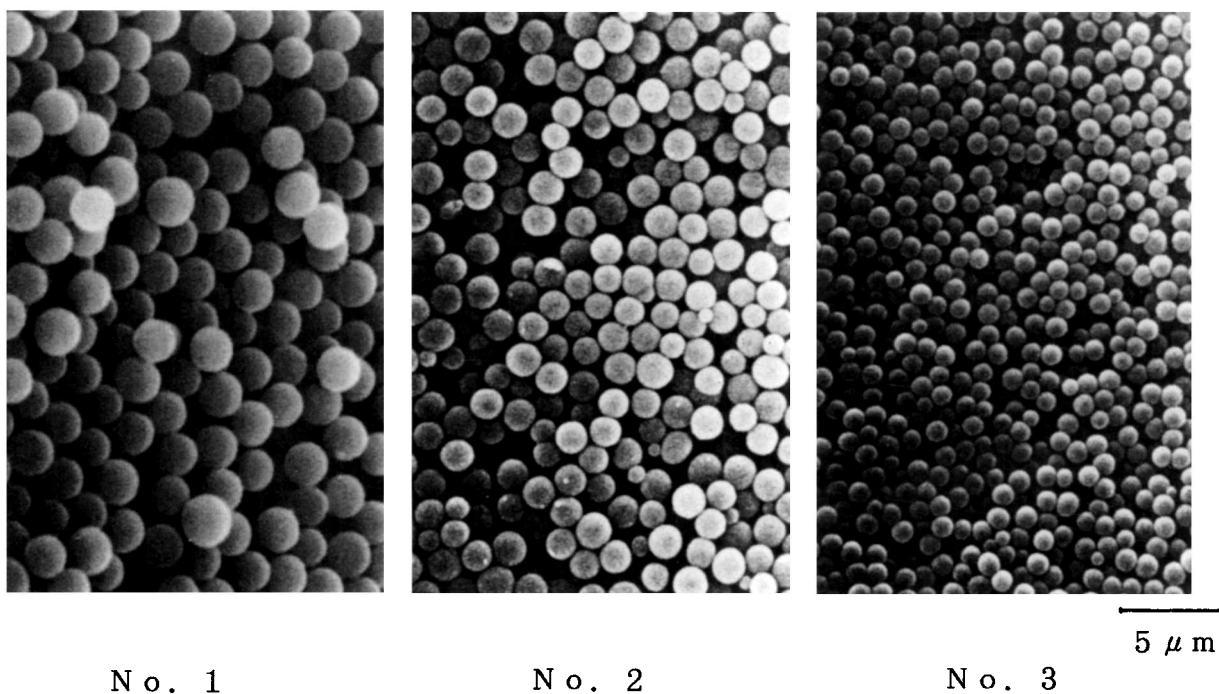
$$D_{\text{max}} (\mu\text{m}) = 0.9388 P_j^{-1} \quad (2)$$

Gurley Air Permeability

Gurley air permeability ($\text{s}/100 \text{ mL air}$) is defined as the time during which 100 mL of air permeates through a microporous PP sheet under pressure, $0.879 \text{ g}/\text{mm}^2$ (JIS P 8117).

Tensile Strength at Yield and Elongation to Break

Microporous PP sheets (length, 150 mm, and width, 25 mm) were prepared and the length direction was just parallel to the MD or TD. The measurement was carried out using an Autograph IS-2000 from



No. 1

No. 2

No. 3

Figure 1 SEM photographs of polymethylsilsesquioxane fillers nos. 1–3. Mean particle size: no. 1, 2 μm ; no. 2, 1.3 μm ; and no. 3, 0.8 μm .

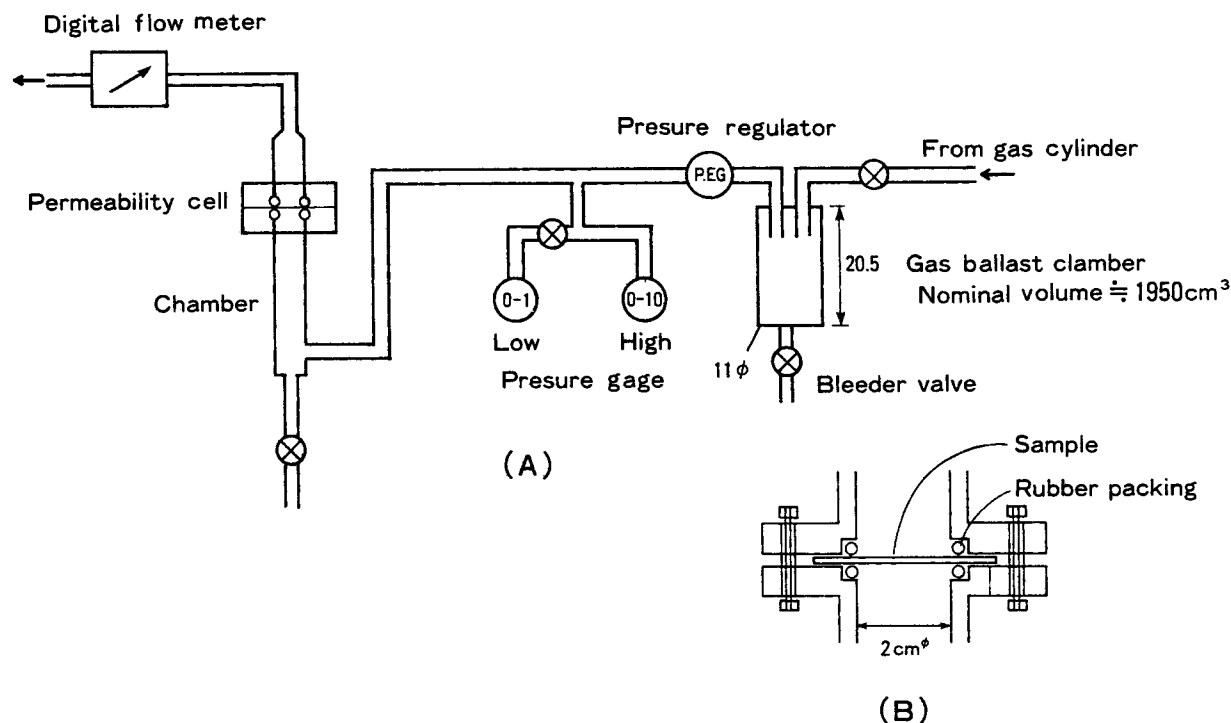


Figure 2 (A) Apparatus and (B) cell to measure gas permeability.

Shimazu Seisakusho Co. The test conditions were temperature, 23°C; relative humidity, 50%; and pulling rate, 200 mm/min. Three measurements were done for each sample and the average values are shown (JIS K-7127).

Tear Strength

Microporous PP sheets (length, 150 mm, and width, 40 mm) were prepared and the length direction was just parallel to the MD or TD. The microporous PP sheets were cut 50 mm from the midpoint of the width edge, just parallel to length direction. The tear strength was measured with a tensile rate of 200 mm/min using an Autograph IS-2000 from Shimazu Seisakusho Co. (JIS P 8116).

Water-resistant Pressure

A microporous PP sheet was set in the upper part of a cylindrical vessel using a flange and the vessel was filled with water. While raising the water pressure at the rate of 60 ± 3 cmH₂O/min, the water pressure was measured as the water-resistant pressure (mmH₂O) when the first water droplet appeared onto the sheet surface (JIS L-1092).

N₂ Gas Permeability

The sample was set between the fringes sealed with rubber packing at an effective diameter of 20 mm, as shown in Figure 2. N₂ gas was supplied into the chamber through a pressure regulator (accuracy, 0.02 kg/cm²). N₂ gas flux (J) was measured by a digital flowmeter, Model 2500 SS, from Sōgō Rikagaku Industry Co., when inlet pressures (P_i) were 1.5, 1.75, and 2.0 kg/cm² and outlet pressure (P_o) was 1 kg/cm². Mean pressure (\bar{P}) was calculated by the following equation:

$$\bar{P} = (P_i + P_o)/2 \quad (3)$$

Determination of Pore Structure

The micropore structure of the PP sheets and the gas permeability was measured as described previously using the apparatus shown in Figure 2.¹⁰ Yasuda and Tsai¹² and Cabasso et al.¹³ studied gas permeation through various millipore filters and polysulfone membrane and derived the following equations:

$$J = K\Delta P l^{-1} \quad (4)$$

where J is the gas flux (cm³/cm² s); K , the per-

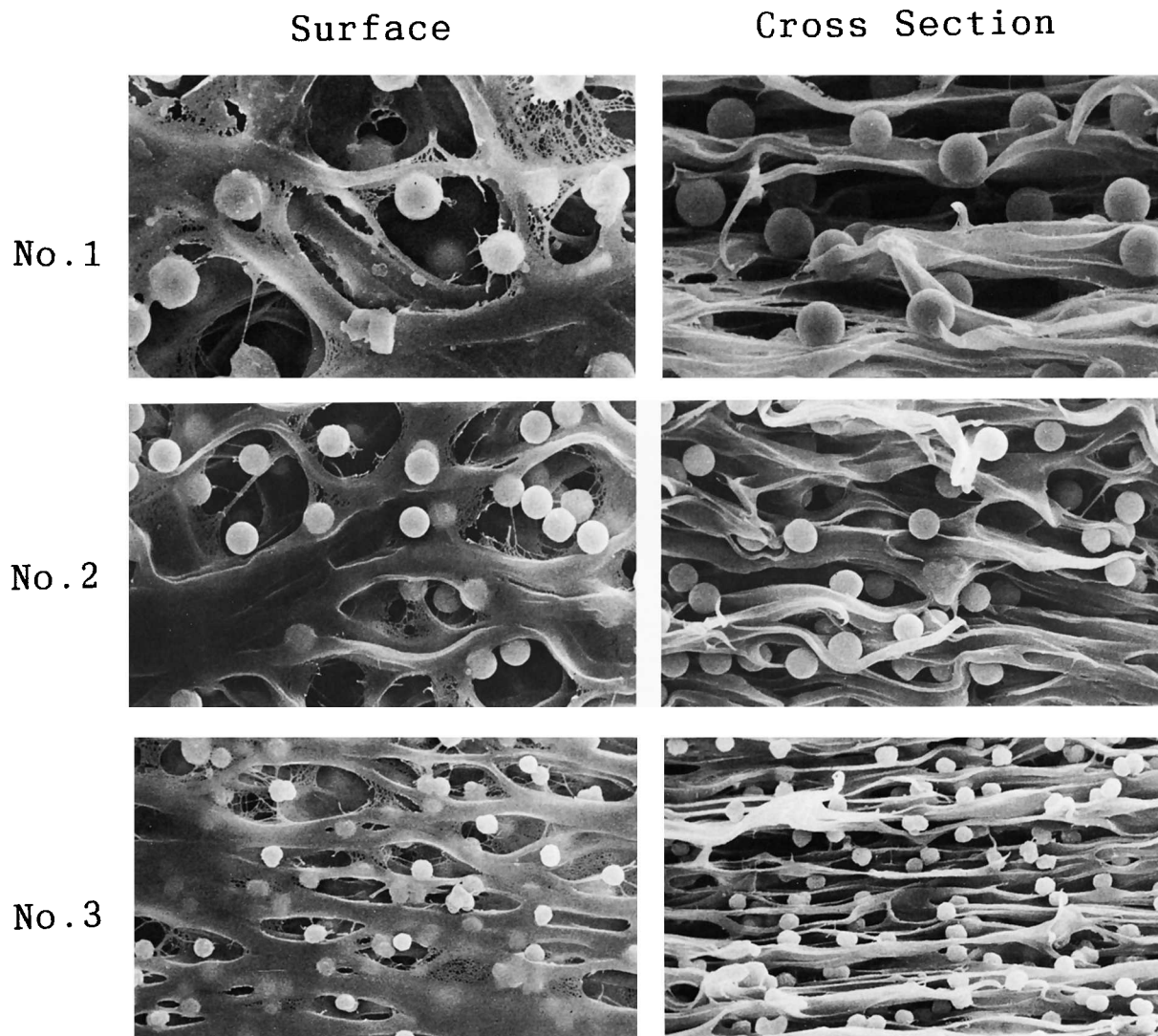


Figure 3 SEM photographs of biaxially stretched pp microporous sheet. Mean particle size of polymethylsilsesquioxane filler: no. 1, 2 μm ; no. 2, 1.3 μm ; and no. 3, 0.8 μm .

meability coefficient (cm^2/s); ΔP , the pressure difference across the sample (kg/cm^2); and l , the thickness of a sample (cm). The gas permeability coefficient (K) is determined as follows:

$$K = lP_0Q(A\Delta P)^{-1} \quad (5)$$

where Q is volume flow rate of N_2 gas (cm^3/s), and A , the effective area of the sample (6.6 cm^2).

The permeability coefficient (K) of a microporous sheet can be shown as follows:

$$K = K_0 + B_0 \cdot \eta^{-1} \cdot \bar{P} \quad (6)$$

where K_0 is the Knudsen permeability coefficient

(cm^2/s); B_0 , the geometric factor of the sheet; and η , the viscosity of N_2 gas ($1.75 \times 10^{-4} \text{ dyne s}/\text{cm}^2$ at 20°C). K_0 and B_0 can be estimated from the plot of K to \bar{P} .

The porosity of the sheet (ϵ) and the tortuosity factor of pore (q) can be related to K_0 and B_0 as follows:

$$K_0 = (4/3)(\delta/k_1)(\bar{v}/q^2)\epsilon m \quad (7)$$

$$B_0 = m^2/k(\epsilon/q^2) \quad (8)$$

where δ/k_1 and k are constant (0.8 and 2.5, respectively) as estimated by Carman;¹⁴ and m , the equivalent pore size as shown below.

Table II Properties of the Microporous PP Sheets

Particle Size of Filler (μm)	Stretching Ratio		Thickness (μm)	Porosity	D_{max} (μm)
	MD	TD			
2.0	4	—	35	0.40	0.61
2.0	4	2	25	0.71	1.56
1.3	4	—	35	0.46	0.46
1.3	4	2	25	0.78	0.78
0.8	4	—	37	0.44	0.44
0.8	4	2	25	0.77	0.59

Thickness of base sheet: 95 μm .

The average molecular velocity of a gas (\bar{v} ; molecular weight, M) is shown as follows:

$$\bar{v} = (8RT/\pi M)^{0.5} \quad (9)$$

The equivalent pore size (m) can be calculated by combining eqs. (7)–(9):

$$m = (16/3)(B_0/K_0)(2RT/\pi M)^{0.5} \quad (10)$$

Thus, eq. (11) can be derived for measurement with N_2 gas at 20°C:

$$m = 1.256 \times 10^5 (B_0/K_0) \quad (11)$$

Furthermore, the following equations are derived from eqs. (7) and (9) to estimate effective porosity (ε/q^2) and tortuosity factor of pore (q):

$$\varepsilon/q^2 = 2.5B_0/m^2 \quad (12)$$

$$q = 0.63m(\varepsilon/B_0)^{0.5} \quad (13)$$

Also, the apparent pore number (n) can be obtained assuming that the pores are cylindrical and perpendicular to the sheet surface:

$$n = \varepsilon/\pi m^2 \quad (14)$$

RESULTS AND DISCUSSION

The properties of the polymethylsilsesquioxane microspheres used to prepare these PP microporous composite sheets are collected in Table I and shown in Figure 1, and Table II records the physical properties of the microporous PP sheets obtained thereby. These data show that stretching in MD and successive stretching in the TD cause the thickness to decrease and the porosity to increase as expected. Both tendencies are independent of the size of the filler particle. On the other hand, the maximum pore size (D_{max}) increases by the successive stretching in the TD. Furthermore, D_{max} increases with increase in the size of the filler particle. Some physical properties of the microporous PP sheets are collected in Table III, which shows that the Gurley's air permeability, water-resist pressure, and tear strength in the TD vary inversely with the particle size of the filler. However, the other properties are not affected by this variable.

Here, it is interesting and noteworthy that the tendencies described above are dependent mainly on the size of the filler particle since the fillers have relatively uniform particle sizes. These results are supported by scanning electron micrographs of the surfaces and the cross sections of the microporous PP sheets (Fig. 3), which show that filler particles are well dispersed in the stretched PP texture. The cross sections parallel to the MD show a layered structure of the PP texture, which becomes finer with decreasing size of the filler particle, which is

Table III Some Properties of Microporous PP Sheets in Relation to Practical Application

Particle Size of Filler (μm)	Gurley's Air Permeability (s/100 mL)	Water Resist Pressure (mmH ₂ O)	Tensile Strength (kg/mm ²)	Elongation (%)	Tear Strength (g/mm)
2.0	25	9,250	MD 3.2	37	23
			TD 1.3		
1.3	44	15,500	MD 4.7	69	25
			TD 1.2		
0.8	90	18,000	MD 4.6	52	20
			TD 1.4		

Stretching degree: $\times 4$ in the MD and $\times 2$ in the TD.

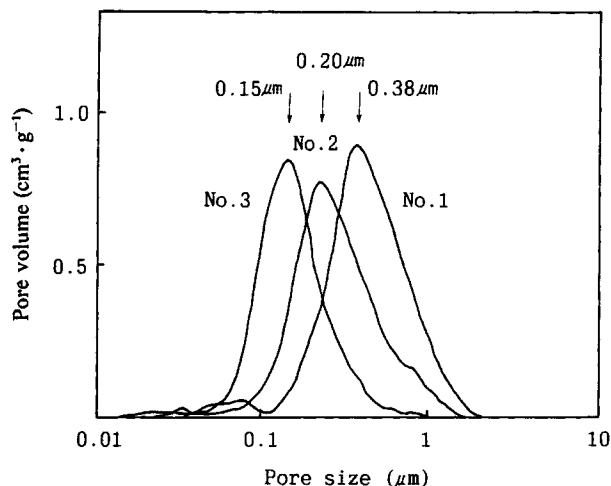


Figure 4 Pore-size distribution of biaxially stretched microporous sheet. Nos. correspond to the samples shown in Table I.

characteristic of microporous composite PP sheets. Figure 4 shows the pore-size distribution curves of the microporous PP sheets, which are of similar shape. The pore size at the peak of the curve becomes larger with increasing size of the filler particle. The reason why the layered structure is formed can be explained as follows: The base sheets are two-dimensionally stretched in the MD and then in the TD, so minute void formation occurs by peeling at the interface between the PP phase and the surface of the filler particles in the stretching directions. Accordingly, the stretched PP phase tends to form fine layers parallel to the stretching plane direction and, furthermore, the fine layers are three-dimensionally interconnected with the fine PP strands. The smaller the particle size of polymethylsilsequioxane filler, the smaller the distance between the layers.

Figure 5 shows the dependency of N_2 gas flux (J) through the microporous PP sheets on the pressure difference (ΔP). The larger the pressure difference, the larger the N_2 gas flux. There is the linear relations between the pressure difference and the N_2 gas flux. Permeability coefficients (K) can be obtained from the slopes of the lines shown in Figure 5. Figure 6 shows the relation between mean pressure (\bar{P}) and the permeability coefficient (K). The larger the mean pressure, the larger the permeability coefficient. The smaller the size of filler particle, the smaller the permeability coefficient. The Knudsen permeability coefficient (K_0) and B_0/η can be obtained from the intercepts on the vertical axis and the slopes of the linear lines shown in Figure 6, respectively. Figure 7 shows the estimated values of

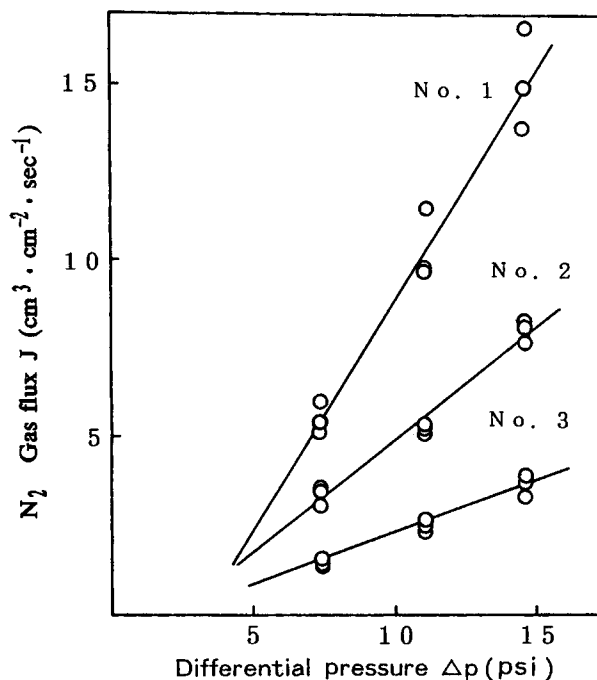


Figure 5 Dependency of N_2 gas flux (J) through the microporous sheet on pressure difference (ΔP).

K_0 and B_0/η in relation to the size of the filler particle. As the filler particle becomes larger, K_0 and B_0/η increase, indicating the tendency of the pore

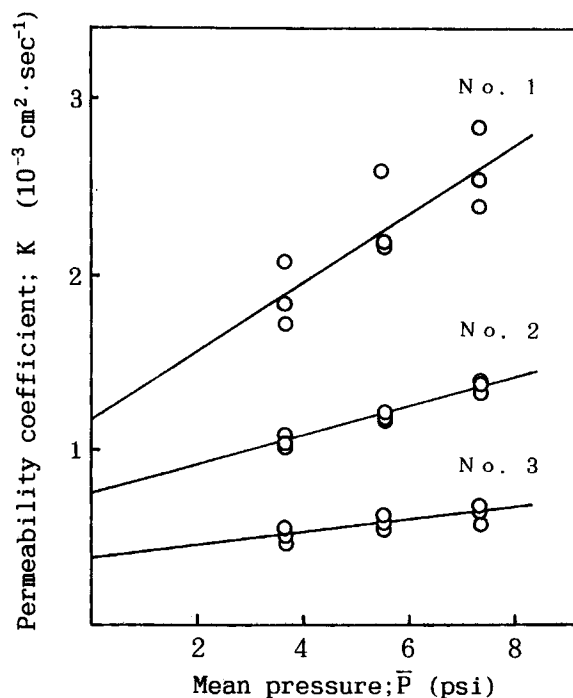


Figure 6 Relationship between mean pressure (\bar{P}) and permeation coefficient (K).

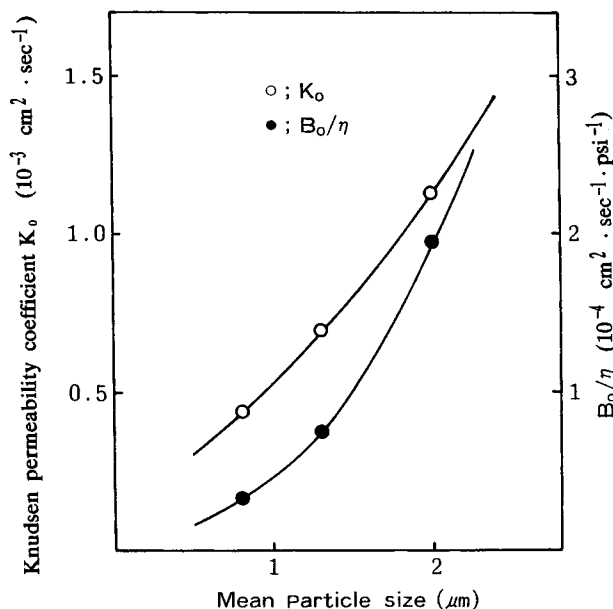


Figure 7 Relationship of permeability coefficient (K_0) and (B_0/η) to the mean particle size of fillers.

becoming larger. The equivalent pore size (m), through which N_2 gas permeates, is estimated from eq. (11) and the value of B_0/η . Figure 8 shows the comparison of the relations between the mean size of the filler particle and the pore size determined by various methods. All the curves show clearly that the smaller the size of the filler particle the smaller the pore-size distribution. Figure 9 shows that the pore number decreases inversely with the mean particle size of the filler.

Figure 10 shows the dependency of the effective porosity (ϵ/q^2) and the tortuosity factor (q) on the mean particle size of the filler, determined by eqs. (13) and (14). As the size of the filler particle becomes smaller, the effective porosity increases and the tortuosity factor decreases. In this study, the fillers used are of the spheric polymethylsilsesquioxane with relatively uniform size (mean particle size, 0.8–2 μm). Therefore, the smaller the particle size of the filler, the more the splitting point of the PP phase on the particle surface by the uniaxial stretching (in the MD) of the base sheets. Accordingly, the resultant PP texture becomes finer with decreasing the particle size, and it probably causes the decrease of the effective porosity and the increase of the tortuosity factor. On the other hand, when the amorphous CaCO_3 fillers with relatively wider particle-size distribution (mean particle size, 0.8–3 μm) were used, the effective porosity and the tortuosity factor were $4\text{--}11 \times 10^{-4}$ and 36–40, respectively, as shown in the previous paper.¹⁰ Both the

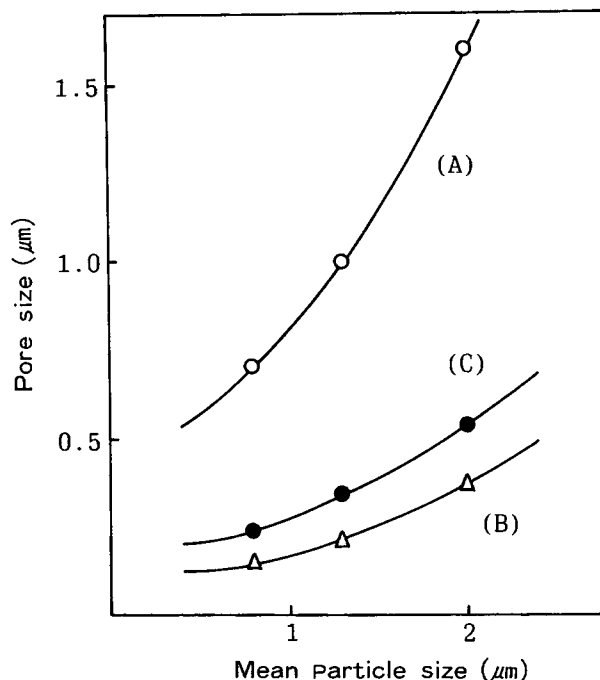


Figure 8 Comparison of the relations between mean particle size of polymethylsilsesquioxane filler and pore size determined by various methods: (A) maximum pore size; (B) pore size at peak position in pore distribution curve in Figure 4; (C) equivalent pore size determined by permeability measurement.

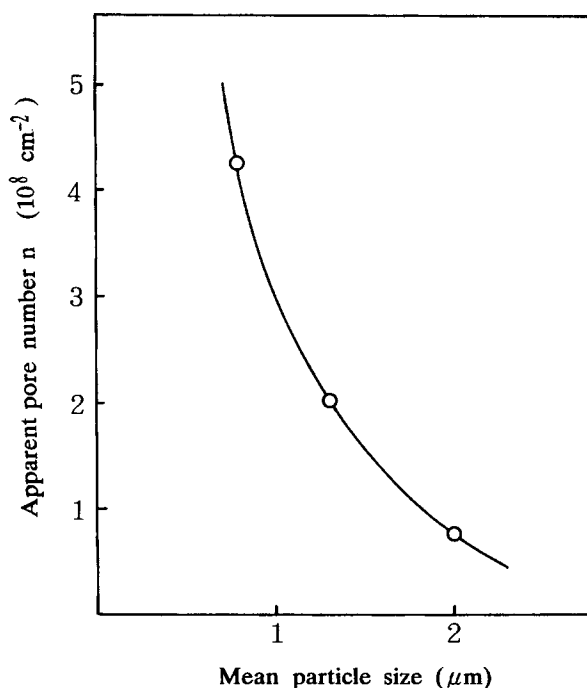


Figure 9 The relation between the mean particle size of the filler and the apparent pore number of microporous sheet.

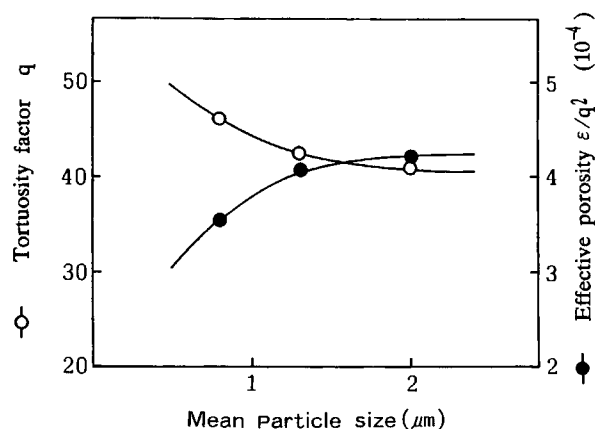


Figure 10 Dependence of effective porosity (ϵ/q^2) and tortuosity factor (q) on mean particle size of fillers.

effective porosity and the tortuosity factor in this study are similar to those described above. However, the dependencies of the effective porosity and the tortuosity factor on the particle size and shape of the filler used, the particle-size distribution, and the affinity of the particle surface with PP are not clear yet, so further investigation should be carried out in the future.

CONCLUSION

Microporous polypropylene sheets can be prepared by biaxially stretching polypropylene sheets containing spheric polymethylsilsequioxane filler with relatively narrow particle-size distribution. Some properties and the structural features of the resultant microporous sheets are investigated in relation to the particle size. With increasing the particle size, the pore size and the effective porosity increase and

the tortuosity factor decreases. However, the dependency of the effective porosity and the tortuosity factor on the properties of various fillers used are still obscure and should further be investigated in the future.

REFERENCES

1. S.-T. Hwang and K. Kammermeyer, *Membranes in Separation*, Wiley, New York, 1973.
2. H. K. Lonsdale, *J. Membr. Sci.*, **10**, 81 (1982).
3. H. S. Bierenbaum, R. B. Isaacson, M. L. Druin, and S. G. Plovon, *Ind. Eng. Chem. Prod. Res. Dev.*, **13**, 1 (1974).
4. M. A. Islam and A. Dimov, *J. Appl. Polym. Sci.*, **45**, 1035 (1992).
5. Y. Mizutani, K. Kusumoto, M. Nishimura, and E. Asada, *J. Membr. Sci.*, **42**, 233 (1989).
6. Y. Mizutani, K. Kusumoto, M. Nishimura, and T. Nishimura, *J. Appl. Polym. Sci.*, **39**, 1087 (1990).
7. S. Nakamura, K. Okamura, S. Kaneko, and Y. Mizutani, *Kobunshi Ronbunshu*, **48**, 463 (1991).
8. S. Nakamura, K. Okamura, and Y. Mizutani, *Kobunshi Ronbunshu*, **48**, 491 (1991).
9. S. Nagō, S. Nakamura, and Y. Mizutani, *J. Electron Microsc.*, **41**, 107 (1992).
10. S. Nagō, S. Nakamura, and Y. Mizutani, *J. Appl. Polym. Sci.*, **45**, 1527 (1992).
11. S. Nakamura, S. Kaneko, and Y. Mizutani, to appear.
12. H. Yasuda and J. T. Tsai, *J. Appl. Polym. Sci.*, **18**, 805 (1974).
13. I. Cabasso, K. Q. Robert, E. Klein, and J. K. Smith, *J. Appl. Polym. Sci.*, **21**, 1883 (1977).
14. P. G. Carman, *Flow of Gas through Porous Media*, Butterworth, London, 1956, p. 77.

Received February 22, 1993

Accepted May 7, 1993